Energy Proceedings
Vol 38, 2024
ISSN 2004-2965

The Lifetime Carbon Footprint of Lithium-Ion Battery Systems in Exemplary Applications

Anupam Parlikar[1],*, Nils Collath[1], Benedikt Tepe[1], Holger Hesse[2], Andreas Jossen[1]

1 Technical University of Munich (TUM), School of Engineering and Design, Department of Energy and Process Engineering, Chair of Electrical Energy Storage Technology (EES), Arcisstr. 21, 80333 Munich, Germany

2 Kempten University of Applied Sciences, Faculty of Mechanical Engineering, Institute for Energy and Propulsion Technologies, Bahnhofstr. 61, 87435 Kempten, Germany
* Corresponding Author: anupam.parlikar@tum.de

ABSTRACT

Energy storage plays a crucial role in the energy transition. Lithium-ion cell technology is the leading energy storage technology today across both the major pillars of the energy sector: mobility and electricity. Lithium-ion batteries are deployed in electric vehicles spanning all segments, and in stationary battery energy storage systems to provide a variety of both grid-connected and off-grid services. While there are no direct emissions due to the use of this technology, the carbon footprint of a Lithium-ion battery comprises of indirect emissions in its production, its operation, and recycling phases. Repurposing of decommissioned automotive batteries in 'second-life' stationary applications is a widely discussed concept to meaningfully extend the battery lifecycle before recycling. In this work, the lifecycle carbon footprint of Lithium-ion batteries operating in three overarching pathways is quantified simulatively with open-source python-based energy system and battery system simulation programs. These pathways are – i) automotive application (A), ii) stationary application (S), and iii) automotive application followed by a second-life stationary application (AS). From the dual perspective of decarbonization and resource efficiency, it is essential to identify the most effective lifecycle pathways for battery system applications. The metric 'Levelized Emissions of Energy Supply', LEES, is used to compare the scenarios. It is found that under the considered assumptions and simulation conditions, the S pathway performs the best, followed by the cascaded AS pathway. The automotive pathway A has the highest LEES value.

Keywords: Battery Electric Vehicle, Second-Life Battery System, Battery Energy Storage System, Electric Vehicle Battery, Levelized Emissions of Energy Supply (LEES), Carbon Footprint

NOMENCLATURE

Abbreviations	
BESS	Battery Energy Storage System
BOL	Beginning-of-Life
CI	Carbon Intensity
EOL	End-of-Life
EV	Electric Vehicle
EVB	Electric Vehicle Battery
GWP	Global Warming Potential
LCA	Lifecycle Analysis
LEC	Load Energy Consumption
LEES	Levelized Emissions of Energy Supply
LFP	Lithium Iron Phosphate
NMC	Nickel Manganese Cobalt Oxide
SOC	State of Charge
SOCI	State of Carbon Intensity
SOH	State of Health
Symbols	
ε	Emissions
E	Energy
P	Power
Subscripts	
A	Automotive application
S	Stationary application
t	At time t
Superscripts	
ch	Charge
dch	Discharge
el	Electronics
gr	Grid section
hsg	Housing
op	Operation phase
prod	Production phase

This is a paper for 15th International Conference on Applied Energy (ICAE2023), Dec. 3-7, 2023, Doha, Qatar.

repurp	Repurposing
trans	Transport

1. INTRODUCTION

Lithium-ion battery technology is the primary enabler of the recent advances in electromobility and the driving force behind its adoption globally. The global Electric Vehicle (EV) stock was 26 million in 2022, which is five times the number of EVs on the road in 2018 [1]. EV volumes are only expected to rise in all major global regions due to favorable policy incentives and technology improvements. Lithium-ion Battery Energy Storage Systems (BESSs) are also now a mature energy storage technology for the provision of grid-related services [2]. The demand for BESSs in grid applications has risen manifold over the recent past and is also expected to rise further [3]. Typical stationary BESS applications include residential self-consumption increase, provision of Frequency Containment Reserve (FCR), and peak load shaving [4].

Due to a multitude of cell-internal aging mechanisms, lithium-ion batteries are subject to degradation, which among others leads to a decrease in cell capacity and an increase of the cell's internal resistance [5]. In the case of automotive battery packs, these gradually become unfit for service due to capacity and power fade. This leads to reduced range and acceleration/regenerative braking capabilities. The extent of degradation depends on the operating conditions (state-of-charge, charge/discharge-rate, etc.), and multiple modelling approaches exist to quantify battery degradation as a functions of a battery's operating conditions, which can be classified into empirical, semi-empirical and physicochemical models [6]. A common assumption is that after a certain extent of aging, for example at a remaining capacity, or State of Health (SOH) of 70 % or 80 %, the battery reaches its end-of-life upon which it can no further be used, since battery cells often show significantly accelerated aging behavior past this point [7,8]. Furthermore, the reduced capacity and increased resistance negatively affect the economic [9] benefit gained from operating a BESS in the respective application.

Decommissioned automotive battery packs can be redeployed in stationary applications where the reduced energy and power densities are not as critical. The battery packs are collected at vehicle dealerships and other locations and are sent to battery repurposing centers for testing and integration in stationary BESSs [10]. Fig. 1 depicts the typical lifecycle of a Lithium-ion battery. Three possible lifecycle pathways for Lithium-ion batteries are discussed in this work. The first pathway, A, considers the use of batteries in an automotive application, followed by recycling on reaching the End-of-Life (EOL) criterion. The second pathway, S, consists of the use of these batteries in an exemplary stationary application (such as the provision of frequency Containment Reserve (FCR)), followed by recycling on reaching the EOL criterion. The third pathway, AS, is the so-called cascaded lifecycle pathway, which consists of a first-use phase in the automotive application, repurposing for use in the chosen second-life stationary application, and finally recycling. The present work investigates these three pathways from a carbon footprint/emissions perspective. The three pathways are simulated to obtain and compare their lifetime carbon footprints. Section 2 describes the simulation programs and the modeling procedure to compute the lifetime emissions. Section 3 describes the simulation setup, scenarios, and discusses the results. Section 4 briefly concludes with a summary of the results and provides a short outlook.

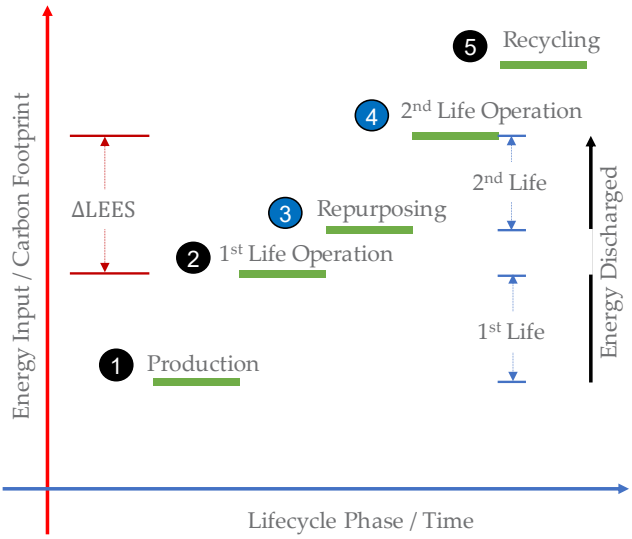

Figure 1: Qualitative depiction of the lifecycle of Lithium-ion battery systems, and the associated carbon footprint.

2. METHODS

This section describes the simulation tools used to model the localized energy system and the battery system in both automotive and stationary applications. The calculation methodology for the emissions in each lifecycle phase is also briefly described here.

2.1 Simulation Tool: Energy System Network (ESN)

The energy system simulation program *Energy System Network (ESN)* is used to model the scenarios

considered in this work. ESN is capable of modelling localized energy systems, consisting of generation, storage, grid, and load components. The program captures the energy flows and lifetime emissions associated with each component included within the specified system boundaries. This program is used to model energy system scenarios within which the battery lifecycle pathways are embedded. ESN [1] is already available to the wider scientific community as an open-source program, while the associated publication is currently under review [11].

2.2 Simulation Tool: Simulation of Stationary Energy Storage Systems (SimSES)

Battery system modelling in ESN is achieved through seamless coupling with the open-source python program, *Simulation of Stationary Energy Storage Systems (SimSES)* [2]. SimSES is capable of modelling a battery system from the cell-level up to the ambient environment in which it is placed. [12]

2.3 Modelling an automotive application

The modeling procedure of an automotive battery application is presented in this section. Fig. 2 depicts the automotive battery system installed in an EV. The chosen system boundaries include the EV battery (EVB) system itself, but not the external power electronics in the charging infrastructure.

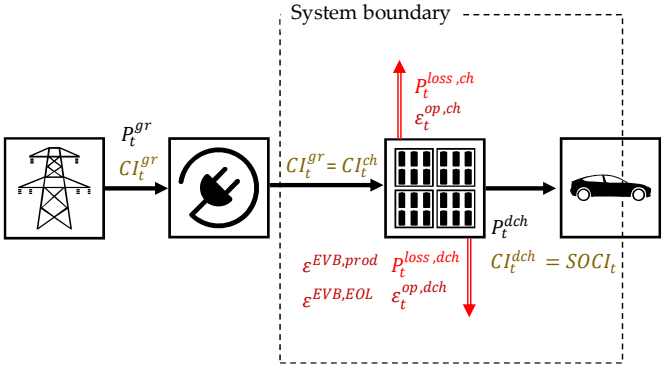

Figure 2: Modelling an automotive application and its system boundaries. The EVB includes power electronics and other peripheral components.

The GWP footprint of the automotive application, i.e., of the system contained within the system boundaries, as depicted in fig. 2 comprises of the production phase, the operation phase, and the EOL phase emissions of all included components. In addition, the Load Energy Consumption (LEC) emissions associated with the consumption of energy are also considered [13]. We use a versatile metric, the Levelized Emissions of Energy Supply (LEES) to capture the effect of all these quantities on the carbon footprint of the energy system contained within the system boundaries (eq. 1) [14].

$$LEES_A = \frac{\varepsilon_A^{EVB,prod} + \varepsilon_A^{EVB,op} + \varepsilon_A^{EVB,EOL} + \varepsilon_A^{LEC}}{E_A^{dch}} \quad (1)$$

2.4 Modelling a stationary application

In this section, the modeling procedure for a stationary battery application is presented. Fig. 3 depicts the battery installed in a grid-connected stationary application. The chosen system boundaries include the BESS itself, but not its coupling with the grid, which may also include a transformer. Analogous to the automotive application discussed earlier, the GWP footprint of the system contained within the system boundaries includes the production phase, operation phase, and EOL phase emissions of all components. Additionally, the LEC emissions on account of energy consumption are also calculated.

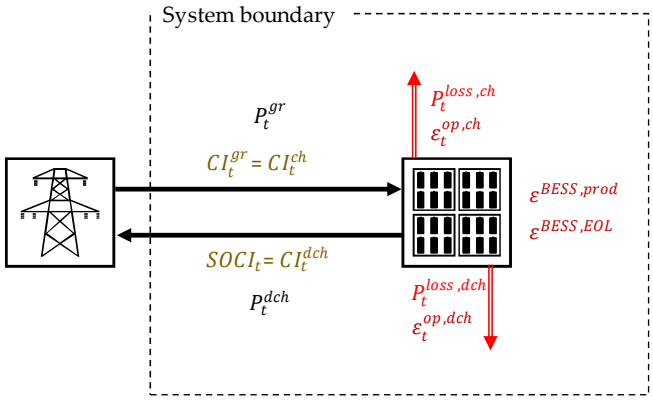

Figure 3: Modelling a stationary application and its system boundaries. The BESS includes the power electronics and other peripheral components, except the grid coupling.

These quantities can be captured in the LEES metric (eq. 2). As there is no explicit energy consuming load in a purely grid-connected battery application, the energy discharged back to the grid is treated as the consumed energy.

$$LEES_S = \frac{\varepsilon_S^{BESS,prod} + \varepsilon_S^{BESS,op} + \varepsilon_S^{BESS,EOL} + \varepsilon_S^{LEC}}{E_S^{dch}} \quad (2)$$

[1] ESN code repository: https://gitlab.lrz.de/open-ees-ses/energy_system_network

[2] SimSES code repository: https://gitlab.lrz.de/open-ees-ses/simses

2.5 Production phase

The production phase of a Lithium-ion BESS is energy intensive and is responsible for GHG emissions. These emissions are due to the production of Lithium-ion cells, power electronics modules, and other components. These emissions are assigned to the lifecycle of the BESS. The exact BESS configuration and the energy mix available at the production location both play an important role in the determination of these emissions. A literature-based streamlined LCA study of a BESS with cells of the Lithium Irion Phosphate (LFP) chemistry has been compiled in a previous study, and is deemed sufficient for the purpose of this work [14]. The production phase footprint for each of the chosen configurations in this study is discussed in section 3.

2.6 Operation phase

The operation phase emissions of battery systems are calculated from the energy conversion losses during the charge and discharge processes. These emissions are indirect emissions, which occur during the generation of the lost energy. As these emissions are caused due to the presence of the battery system in the energy system, they are allocated to the operation phase of the battery. The operation emissions in the charge process at each instant are given by the product of the carbon intensity of the charging energy, the charging loss power, $P_t^{ch,loss}$, and the simulation timestep, Δt. The carbon intensity of the charging energy is equal to the grid carbon intensity, CI_t^{gr}, in the current study, as no other power generation sources are present in the chosen configurations. The operation emissions at each instant during the discharge process are equal to the product of the State of Carbon Intensity (SOCI) at time t, $SOCI_t$, the discharge loss power, $P_t^{dch,loss}$, and the simulation timestep, Δt. The state variable SOCI has been introduced and extensively discussed in a previous work [13]. The emissions over the entire simulation period are obtained by summing up the emissions over all timesteps (eq. 3). The operation phase emissions are a function of the carbon intensity of the grid energy, and the energy losses during charging and discharging.

$$\varepsilon^{batt,op} = \Sigma\left(CI_t^{gr} \cdot P_t^{ch,loss} + SOCI_t \cdot P_t^{dch,loss}\right)\Delta t \qquad (3)$$

2.7 End-of-Life (EOL) phase

The battery reaches End-of-Life (EOL) due to either having reached a preset EOL criterion, such as a set value of the remaining capacity, beyond which a battery is not expected to perform reliably or safely, or if the required performance is not being met. Such batteries are sent to recycling facilities to recover metals and to suitably process other materials. Representative EOL phase emissions values have also been determined in a previous study as part of the literature-based streamlined LCA [14]. The EOL phase emissions are negative if materials are recovered and can be reused in the production process. This leads to emissions savings, which are 'credited' as negative emissions values. The EOL phase emissions for the configurations chosen in this study are discussed in section 3.

2.8 Repurposing of automotive batteries

In automotive applications, the battery witnesses a gradual fading of the capacity and power capability due to degradation processes occurring in the cells, as discussed in section 1. These batteries can be repurposed for operation in stationary applications. Additional components are installed to create a stationary BESS. Based on the studied literature, the carbon footprint of the repurposing process, excluding any disassembly and reassembly is found to be around 7.72 kgCO2eq/kWh of nominal battery energy capacity [15]. Two additional transport phases to and from the repurposing are also to be considered in the carbon footprint of the repurposing phase. For the LFP batteries, this amounts to an additional 0.2 kgCO2eq/kWh of nominal battery capacity assuming two transport phases of 200 km in each direction to and from the battery repurposing center [16,17].

3. SIMULATION RESULTS AND DISCUSSION

In this section, the three possible overarching lifecycle pathways for Lithium-ion batteries discussed in section 1 are presented. Exemplary simulations for these three pathways are run using ESN and SimSES. The results of these simulations are presented and discussed in this section.

The three overarching lifecycle pathways for Lithium-Ion batteries are (also depicted in Fig. 4):

1. **A:** Deployment in automotive application followed by recycling on reaching of EOL criterion corresponding to SOH = 60%
2. **S:** Deployment in stationary application followed by recycling on reaching EOL criterion of SOH = 60%
3. **AS:** Deployment in automotive application until SOH = 80% is reached followed by repurposing for deployment in a stationary application, and recycling on reaching SOH = 60%

In the following subsections, the simulation setup and the influencing factors in each of the pathways are discussed.

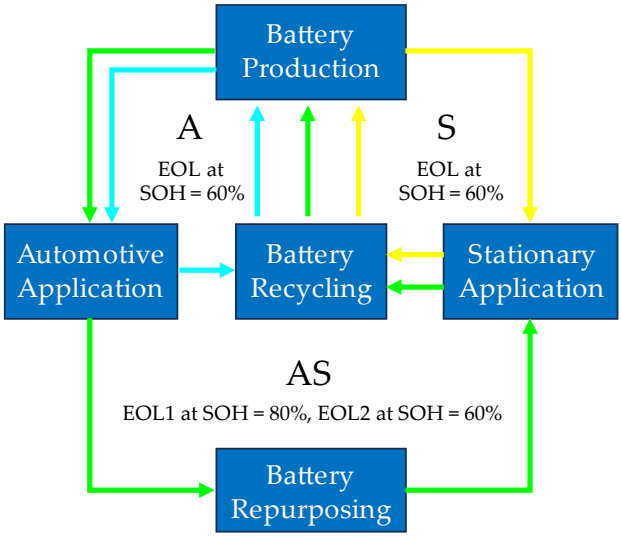

Figure 4: The three possible battery lifecycle pathways: A (Automotive), S (Stationary), and AS (Automotive application followed by a stationary second-life application).

3.1 Pathway A

In pathway A, the carbon footprint of a Lithium-ion battery pack deployed in an automotive application over its entire lifetime is determined. The metric LEES is obtained for the application within the system boundaries as described in section 2. The automotive application is modeled using an EV drive-power profile. This profile has been generated based on driver vehicle utilization behavior using the tool *emobpy* [18]. The application is simulated with a timestep of 900 seconds. This dataset and its attributes have been extensively described in a previous study. The profile and EV battery pack configuration used in this work is based on the drive profile expected for an EV from a leading vehicle manufacturer. [19]

The battery pack configuration is described in Table 1. Table 2 presents the calculated production and EOL phase emissions for the specified battery configuration. The Lithium Iron Phosphate (LFP) cell chemistry is used for the simulations. A parametrized cell model for this chemistry is available in SimSES. In this pathway, cells with SOH = 100% at the Beginning-of-Life (BOL), i.e. new cells, are considered. The EOL criterion signifies the SOH value at which the end of service life is assumed. This criterion is set at SOH = 60% in this pathway. The Lithium-ion cells are recycled at the end of the assumed operation period of 20 years, or on reaching the EOL criterion, whichever is earlier.

Table 1: Automotive application battery pack configuration.

Parameter	Value
Cell type	Lithium Iron Phosphate (LFP)
Cell format	Cylindrical, 26650
Rated energy capacity (kWh)	45
Rated power (kW)	100
Initial State of Health (SOH)	100%
Battery model	R-int Equivalent Circuit Model (ECM) (based on [20,21])
Battery degradation model	Semi-empirical calendric and cyclic (based on [22,23])
Power electronics	AC/DC converter, 5 units (based on [24–26])
Housing type	No Housing assumed
Cooling system	Passive cooling in constant temperature
Ambient conditions	Constant temperature

Table 2: Production and EOL emissions (in kgCO2eq) for the automotive battery pack described in Table 1.

Component	Production	End-of-Life	Source
Cells	7,245	-527	[27,28]
Power Electronics	980	-104	[29,30]
Electronics	619	-90	[29,30]
Total	8,844	-720	

The simulation results and emissions categories in each phase of the battery lifecycle are determined (Table 6). The value of LEES is obtained from the values of the emissions categories presented in the simulation results. The LEES value for the automotive application comes out to 0.7457 $kgCO_2eq/kWh$. The largest contributor to this value are the DEC emissions, followed by the BESS production phase emissions. The BESS operation phase emissions and the grid section operation phase emissions are the third and fourth largest emissions categories. The EOL phase emissions for the BESS are negative due to the carbon credits on account of material recovered from the recycling process. If the EVB were to be decommissioned on reaching SOH = 80%, the LEES value rises to 1.1124 $kgCO_2eq/kWh$. In this case, it takes

around 7 years for the EVB to reach the EOL criterion operating with the simulated load profile. 50% of the production and EOL phase emissions associated with the power electronics are associated with the battery. This is under the assumption that the power electronics can be used in the EV with a battery replacement. The choice of the EOL criterion also affects the LEES value for the pathway.

3.2 Pathway S

In pathway S, the carbon footprint of a Lithium-ion BESS deployed in the chosen stationary grid-connected application – provision of Frequency Control Reserve (FCR) is determined over its entire lifecycle.

Table 3: Stationary application BESS configuration.

Parameter	Value
Cell chemistry	Lithium Iron Phosphate (LFP)
Cell format	Cylindrical, 26650
Rated energy capacity (MWh)	1.62
Rated power (MW)	1.6
Initial State of Health (SOH)	100%
Battery model	R-int Equivalent Circuit Model (ECM) (based on [20,21])
Battery degradation model	Semi-empirical calendric and cyclic (based on [22,23])
Power electronics	AC/DC Converter, 8 units (based on [24–26])
Housing type	20 ft. standard shipping container
HVAC thermal power (kW)	30
Ambient conditions	Berlin

Table 4: Production and End-of-Life emissions (in kgCO2eq) for the stationary BESS described in Table 3.

Component	Production	End-of-Life	Source
Cells	260,805	-18,953	[27,28]
Power Electronics	61,536	-15,125	[29,30]
Electronics	25,477	-3692	[29,30]
Housing	15,720	0	[30]
HVAC	426	0	[31]
Total	363,964	-37,769	

In this application, grid frequency data is used to generate the power target for the BESS based on the grid frequency at the current timestep. This energy management strategy is explained in greater detail in previous publications [4,12]. Grid frequency data of the German grid for the year 2019 is used in this analysis. This data has been obtained from information made available in the public domain by the transmission system operator, TransNetBW [32]. Any potential deviations from the stipulated BESS SOC limits required to provide symmetrical reserves in both the positive and negative directions are corrected by buying/selling energy on the intraday energy markets. The BESS configuration is described in Table 3. Table 4 presents the calculated production and EOL phase emissions for the specified battery configuration.

This application is simulated for a period of 20 years with a downsampled time resolution of 15 minutes (900 seconds), which reduces the number of data points to 35,040 per year, instead of over 31.5 million per year with a time resolution of 1 second [33]. Although this is less accurate than simulating the operation with a time resolution of 1 second, a significant reduction in both the simulation time and the data volumes is achieved.

The LEES value for the application is obtained from the calculated emissions categories in Table 6. The LEES value for the application is 0.5938 $kgCO_2eq/kWh$. The largest contributing category to this value are the DEC emissions, followed by the BESS operation phase emissions, and the BESS production emissions. The grid operation phase emissions constitute the smallest emissions category. The BESS EOL phase emissions are again negative, reflecting the emissions credits on recycling recovered materials.

3.3 Pathway AS

In pathway AS, the carbon footprint of the Lithium-ion battery pack over its lifetime with an automotive 'first-life' application, and a stationary 'second-life' application is calculated. The battery pack is first deployed in an automotive application. After attaining an SOH value of 80%, the battery pack is repurposed for use in a stationary application. The battery is operated in the stationary application until it either reaches the second EOL criterion of 60%, or until a total service duration of 20 years is reached. It is then sent to the recycling facility to recover the metals and other materials used in its construction.

The simulated automotive application is identical to pathway A, with the exception of the EOL criterion, which is set to 80%, and not 60%. Repurposing is carried out between the automotive and stationary applications. It is assumed that the power electronics of the EV remain fit for service with a battery pack replacement, until the

vehicle is scrapped. As the EV could potentially operate two battery packs during its lifetime, 50% of the production and EOL emissions for the power electronics are then allocated to the first life battery application. The stationary application is identical to pathway S, and is simulated until an SOH value of 60% is reached, or when the battery completes a total 20 year operation period. Additional components such as the power electronics, container housing, and air conditioning systems are installed with the repurposed battery packs. In the stationary application, 45 repurposed automotive packs are installed. These 45 packs together possess an effective energy capacity of 1.62 MWh (at SOH = 80%) with an original nominal energy capacity of 2.025 MWh.

Table 5: Battery parameters (simulation results)

Quantity	A	S	A|S	
Start SOH	100%	100%	100%	80%
Mean SOC	97.61%	47.58%	97.87%	47.28%
Mean DOC	18.95%	4.22%	16.85%	3.72%
Total EFCs	945.43	3,953.27	327.53	2,489
Mean SOCI (gCO_2eq/kWh)	458.36	444.94	459.20	442.19
End SOH	65%	76%	80%	72%
Resistance increase	17.44%	46.23%	6.02%	28.81%
Operation duration (years)	20	20	7	13

The LEES value for this cascaded lifecycle pathway is calculated as in eq. 6. Eqs. 4 and 5 present the emissions associated with the battery in automotive and stationary applications. f_A and f_S are factors to determine the share of the production and EOL phase emissions for the peripheral components which are allocated to the automotive and stationary applications respectively. This includes the power electronics (PE), the container housing, and the Heating, Ventilation, Air Conditioning (HVAC) system. In this case, f_A is set to 0.5, as discussed earlier in this section. As the repurposed BESS can be operated in the stationary application for 13 years, f_S is set to 0.65. These factors control the allocation of the emissions for the peripheral components.

$$\varepsilon_A^{EVB} = \varepsilon^{cells,prod} + \varepsilon_A^{el} + f_A \cdot (\varepsilon_A^{PE}) + \varepsilon_A^{EVB,op} + \varepsilon_A^{LEC} \quad (4)$$

$$\varepsilon_S^{BESS} = f_S \cdot (\varepsilon_S^{PE} + \varepsilon_S^{el} + \varepsilon_S^{hsg} + \varepsilon_S^{HVAC}) + \varepsilon_S^{BESS,op} + \varepsilon_S^{LEC} + \varepsilon^{cells,EOL} \quad (5)$$

$$LEES = \frac{\varepsilon_A^{EVB} + \varepsilon^{trans} + \varepsilon^{repurp} + \varepsilon_S^{BESS}}{E_A^{dch} + E_S^{dch}} \quad (6)$$

The LEES value for this pathway is calculated to be 0.6285 $kgCO_2/kWh$. The category-wise emissions results are tabulated in Table 6. In the automotive application, it takes 7 years under the simulated load conditions to reach the EOL criterion of SOH = 80%. In the stationary application, the battery system is in operation for 13 years, and loses a further 8% of capacity. The EOL criterion of SOH = 60% is not reached within this time period.

From the simulated scenarios, it is observed that the LEES value for pathway A is the highest. This is due to the low utilization of the BESS in the automotive application, which sees just over 945 EFCs over the 20-year simulation period (Table 5). The SOH of the battery gradually drops to 65% in this period. In contrast, the LEES value for pathway S is the lowest over the 20-year period. This is attributable to the higher utilization (3953 EFCs) of the BESS over the 20-year simulated duration, despite which the battery reaches SOH = 76%. The evaluation of the pathway AS is more nuanced. The LEES value is lower than that of pathway A, but higher than that of pathway S. In the first phase, i.e., the A phase of the pathway, the BESS is subjected to over 327 EFCs, while in the second phase (S), the BESS is subjected to a further 2489 EFCs. At the end of the second-use phase, the SOH of the battery is 72%.

Table 6: Simulation results with each emissions category (in kgCO2eq), the discharged energy, and LEES values.

Emissions Category	A	S	A|S	
Production phase (BESS)	8,844.26	363,963.98	8,354.18 (x 45)	54,905.71
Operation phase (BESS)	2,865.12	418,102.75	982.44 (x 45)	255,708.11
Operation phase (grid section)	409.42	63,995.52	142.24 (x 45)	40,157.15
Repurposing	0	0	0	15,633
Transport	0	0	0	406.22
DEC emissions	17,180.82	2,717,493.62	5,964.88 (x 45)	1,711,802.73
EOL phase (BESS)	-720.19	-37,769.34	-668.20 (x 45)	-10,470.47
Energy discharged (kWh)	**38,324.60**	**593,7712.52**	**13,282.33 (x 45)**	**3,751,143.71**
LEES ($kgCO_2eq/kWh$)	**0.7457**	**0.5938**	**0.6285**	

In comparison to pathway A, the SOH drop in the pathways S and AS is lower, due to the degradation characteristics of cell, and the load characteristics of the application. The considered LFP cell is especially susceptible to high calendric degradation at higher SOC values. In pathway A, the EVB remains at high SOC values to maintain drive-readiness. In the pathways S and AS, the chosen stationary application – provision of FCR is peculiar as it maintains the BESS in a mid-SOC range, deviating around SOC = 50% as it provides power to counter the grid frequency deviations. As the chosen cell is also especially stable under intense cyclization, the S and AS pathways do not lead to a correspondingly high cyclic degradation, despite the high EFCs it is subjected to. Despite the high total number of EFCs (over 2816) in the automotive and stationary applications, the LEES for the AS pathway remains higher than that for the S pathway. Fig. 5 depicts the LEES values for the three pathways and the contributions of each emissions category to the value.

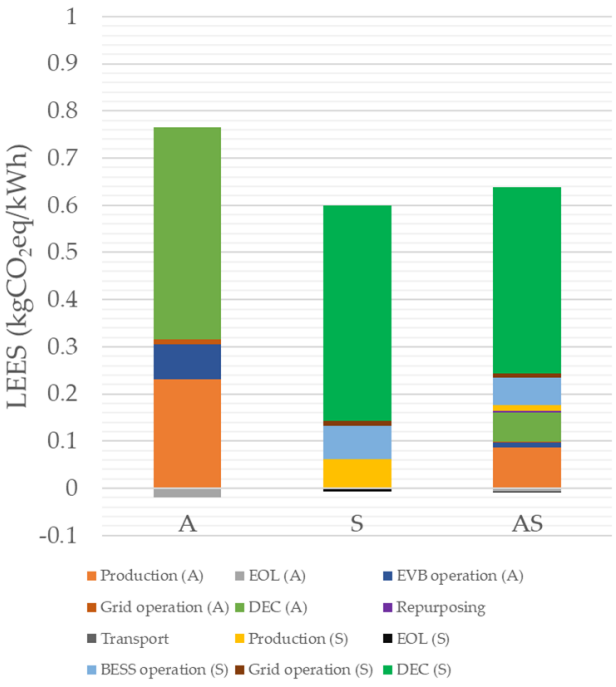

Figure 5: LEES values for the three pathways: A, S, AS. Also depicted are the relative contributions of each emissions category to the LEES value.

4. CONCLUSION AND OUTLOOK

This study investigates the emissions footprint of three possible Lithium-ion battery lifecycle pathways. It is found that for the chosen automotive drive profile and stationary application, the S pathway exhibits the lowest LEES value. The AS cascaded lifecycle pathway fares better than the A pathway. This implies that a cascaded lifecycle pathway (AS) is desirable from the carbon footprint perspective, as compared to the automotive (A) pathway. This also implies that dedicated BESS installations for stationary applications are indispensable, but stationary energy storage can be augmented with repurposed batteries from automotive applications, as the batteries have already been produced, and may as well be deployed in stationary applications to improve their lifetime LEES values. The choice of the EOL criterion in the automotive application is also found to influence the LEES value for the pathway.

The goal of this study is to illustrate the analytical methodology to compare the three possible Lithium-ion battery lifecycle pathways. This study relies on a streamlined LCA based on data published in scientific literature. Primary data is difficult to obtain and remains the biggest hurdle to conducting extremely detailed and precise LCA studies. Access to better data would ensure that this analysis can be updated at a later time. Although the LFP cell model used in this study is known to be especially durable, the cell degradation model used has a square root dependency on time and charge throughput. Consequently, it exhibits slowing degradation with time and charge throughput. The cell can be expected to suffer stronger degradation towards the end of its service life under real-world conditions, which would affect the LEES values. Follow-on analyses to check the sensitivity of cell degradation, the effect of the chosen stationary application on the LEES values are planned. An investigation into the LEES values of a Vehicle-to-Home, or Vehicle-to-X configuration wherein the automotive and stationary applications are serviced within the same timeframe, rather than sequentially as in pathway AS would also be of particular interest. The carbon intensity profile for the German grid in 2019 is used to represent each year in the simulation. This can be thought of as the worst-case scenario since the grid carbon intensity is expected to go down with time as the penetration of renewable energy sources in the energy mix rises.

ACKNOWLEDGEMENT

This research is funded by the German Federal Ministry of Education and Research (BMBF) via the research project *greenBattNutzung* (grant number 03XP0302D). The project is overseen by Project Management Juelich (PtJ). The authors thank Amey Kulkarni for contributing to some aspects of the literature review.

DECLARATION OF INTEREST STATEMENT

The authors declare that they have no known competing financial interests or personal relationships that could have appeared to influence the work reported in this paper. All authors read and approved the final manuscript.

REFERENCES

[1] International Energy Agency (IEA). Global EV Outlook 2023, Paris, France; 2023.

[2] Hesse H, Schimpe M, Kucevic D, Jossen A. Lithium-Ion Battery Storage for the Grid—A Review of Stationary Battery Storage System Design Tailored for Applications in Modern Power Grids: Energies 2017;10(12):2107.

[3] Figgener J, Hecht C, Haberschusz D, Bors J, Spreuer KG, Kairies K-P, Stenzel P, Sauer DU. The development of battery storage systems in Germany: A market review (status 2023). arXiv; 2022.

[4] Kucevic D, Tepe B, Englberger S, Parlikar A, Mühlbauer M, Bohlen O, Jossen A, Hesse H. Standard battery energy storage system profiles: Analysis of various applications for stationary energy storage systems using a holistic simulation framework: Journal of Energy Storage 2020;28:101077.

[5] Vetter J, Novák P, Wagner MR, Veit C, Möller K-C, Besenhard JO, Winter M, Wohlfahrt-Mehrens M, Vogler C, Hammouche A. Ageing mechanisms in lithium-ion batteries: Journal of Power Sources 2005;147:269–81.

[6] Collath N, Tepe B, Englberger S, Jossen A, Hesse H. Aging aware operation of lithium-ion battery energy storage systems: A review: Journal of Energy Storage 2022;55(11):105634.

[7] Collath N, Cornejo M, Engwerth V, Hesse H, Jossen A. Increasing the lifetime profitability of battery energy storage systems through aging aware operation: Applied Energy 2023;348(14):121531.

[8] Attia PM, Bills A, Brosa Planella F, Dechent P, dos Reis G, Dubarry M, Gasper P, Gilchrist R, Greenbank S, Howey D, Liu O, Khoo E, Preger Y, Soni A, Sripad S, Stefanopoulou AG, Sulzer V. Review—"Knees" in Lithium-Ion Battery Aging Trajectories: J. Electrochem. Soc. 2022;169(6):60517.

[9] Uddin K, Gough R, Radcliffe J, Marco J, Jennings P. Techno-economic analysis of the viability of residential photovoltaic systems using lithium-ion batteries for energy storage in the United Kingdom: Applied Energy 2017;206(10):12–21.

[10] Martinez-Laserna E, Gandiaga I, Sarasketa-Zabala E, Badeda J, Stroe D-I, Swierczynski M, Goikoetxea A. Battery second life: Hype, hope or reality? A critical review of the state of the art: Renewable and Sustainable Energy Reviews 2018;93:701–18.

[11] Parlikar A, Tepe B, Möller M, Hesse H, Jossen A. Quantifying the carbon footprint of energy storage applications with an energy system simulation framework - Energy System Network(under review).

[12] Möller M, Kucevic D, Collath N, Parlikar A, Dotzauer P, Tepe B, Englberger S, Jossen A, Hesse H. SimSES: A holistic simulation framework for modeling and analyzing stationary energy storage systems: Journal of Energy Storage 2022;49:103743.

[13] Parlikar A, Schott M, Godse K, Kucevic D, Jossen A, Hesse H. High-power electric vehicle charging: Low-carbon grid integration pathways with stationary lithium-ion battery systems and renewable generation: Applied Energy 2023;333:120541.

[14] Parlikar A, Truong CN, Jossen A, Hesse H. The carbon footprint of island grids with lithium-ion battery systems: An analysis based on levelized emissions of energy supply: Renewable and Sustainable Energy Reviews 2021;149:111353.

[15] Bobba S, Podias A, Di Persio F, Messagie M, Tecchio P, Cusenza MA, Eynard U, Mathieux F, Pfrang A. Sustainability Assessment of Second Life Application of Automotive Batteries (SASLAB): JRC Exploratory Research (2016-2017). Final technical report: August 2018 2018.

[16] Argonne National Laboratory, U.S. Department of Energy. GREET® Model: The Greenhouse gases, Regulated Emissions, and Energy use in Technologies Model. Argonne National Laboratory; 2022.

[17] Ragon P-L, Rodríguez F. CO2 emissions from trucks in the EU: An analysis of the heavy-duty CO2 standards baseline data; 2021.

[18] Gaete-Morales C, Kramer H, Schill W-P, Zerrahn A. An open tool for creating battery-electric vehicle time series from empirical data, emobpy: Scientific data 2021;8(1):152.

[19] Tepe B, Jablonski S, Hesse H, Jossen A. Lithium-ion battery utilization in various modes of e-transportation: eTransportation 2023;18:100274.

[20] Schimpe M, Kuepach ME von, Naumann M, Hesse HC, Smith K, Jossen A. Comprehensive Modeling of Temperature-Dependent Degradation Mechanisms

in Lithium Iron Phosphate Batteries: J. Electrochem. Soc. 2018;165(2):A181-A193.
[21] Schimpe M, Naumann M, Truong N, Hesse HC, Santhanagopalan S, Saxon A, Jossen A. Energy efficiency evaluation of a stationary lithium-ion battery container storage system via electro-thermal modeling and detailed component analysis: Applied Energy 2018;210:211–29.
[22] Naumann M, Schimpe M, Keil P, Hesse HC, Jossen A. Analysis and modeling of calendar aging of a commercial LiFePO4/graphite cell: Journal of Energy Storage 2018;17:153–69.
[23] Naumann M, Spingler FB, Jossen A. Analysis and modeling of cycle aging of a commercial LiFePO4/graphite cell: Journal of Power Sources 2020;451:227666.
[24] Notton G, Lazarov V, Stoyanov L. Optimal sizing of a grid-connected PV system for various PV module technologies and inclinations, inverter efficiency characteristics and locations: Renewable Energy 2010;35(2):541–54.
[25] Schimpe M, Becker N, Lahlou T, Hesse HC, Herzog H-G, Jossen A. Energy efficiency evaluation of grid connection scenarios for stationary battery energy storage systems: Energy Procedia 2018;155:77–101.
[26] Parlikar A, Hesse H, Jossen A. Topology and Efficiency Analysis of Utility-Scale Battery Energy Storage Systems, In: Proceedings of the 13th International Renewable Energy Storage Conference 2019 (IRES 2019).
[27] Baumann M, Peters JF, Weil M, Grunwald A. CO 2 Footprint and Life-Cycle Costs of Electrochemical Energy Storage for Stationary Grid Applications: Energy Technol. 2017;5(7):1071–83.
[28] Mohr M, Peters JF, Baumann M, Weil M. Toward a cell-chemistry specific life cycle assessment of lithium-ion battery recycling processes: J of Industrial Ecology 2020;24(6):1310–22.
[29] Bulach W, Schüler D, Sellin G, Elwert T, Schmid D, Goldmann D, Buchert M, Kammer U. Electric vehicle recycling 2020: Key component power electronics: Waste management & research the journal of the International Solid Wastes and Public Cleansing Association, ISWA 2018;36(4):311–20.
[30] Wernet G, Bauer C, Steubing B, Reinhard J, Moreno-Ruiz E, Weidema B. The ecoinvent database version 3 (part I): overview and methodology: Int J Life Cycle Assess 2016;21(9):1218–30.
[31] Ylmén P, Peñaloza D, Mjörnell K. Life Cycle Assessment of an Office Building Based on Site-Specific Data: Energies 2019;12(13):2588.
[32] TransnetBW. Systemdienstleistungen: Regel-energie Bedarf und Abruf, 2023, https://www.transnetbw.de/de/strommarkt/systemdienstleistungen/regelenergie-bedarf-und-abruf, accessed 1 March 2023.
[33] Hoffmann M, Kotzur L, Stolten D, Robinius M. A Review on Time Series Aggregation Methods for Energy System Models: Energies 2020;13(3):641.